

We are IntechOpen, the world's leading publisher of Open Access books Built by scientists, for scientists

5,500

Open access books available

136,000

International authors and editors

170M

Downloads

Our authors are among the

154

Countries delivered to

TOP 1%

most cited scientists

12.2%

Contributors from top 500 universities



WEB OF SCIENCE™

Selection of our books indexed in the Book Citation Index
in Web of Science™ Core Collection (BKCI)

Interested in publishing with us?
Contact book.department@intechopen.com

Numbers displayed above are based on latest data collected.
For more information visit www.intechopen.com



Thermodynamics of Perovskite: Solid, Liquid, and Gas Phases

Sergey Shornikov

Abstract

The present work is devoted to the review of experimental data on thermodynamic properties of perovskite in the condensed state, as well as the gas phase components over perovskite and its melts at high temperatures.

Keywords: perovskite, thermodynamics

1. Introduction

Calcium titanate (CaTiO_3) or perovskite was found by Rose [1] in the Ural Mountains in 1839 and named after the Russian Statesman Count Lev Perovski. Perovskite is a relatively rare mineral, which is a promising material for use as matrices for safe long-term storage of actinides and their rare earth analogs that are present in radioactive waste [2]. It is of particular interest for petrology and cosmochemical research as a mineral which is a part of refractory Ca-Al inclusions often found in carbonaceous chondrites, which are the earliest objects of the solar system with unusual isotopic characteristics [3–5].

In addition to perovskite, two more calcium titanates, $\text{Ca}_3\text{Ti}_2\text{O}_7$ [6] and $\text{Ca}_4\text{Ti}_3\text{O}_{10}$ [7], melting incongruently, were found in the CaO-TiO₂ system. The other calcium titanates, Ca_4TiO_6 [8], Ca_3TiO_5 [9], $\text{Ca}_8\text{Ti}_3\text{O}_{14}$ [8, 10], Ca_2TiO_4 [9], $\text{Ca}_5\text{Ti}_4\text{O}_{13}$ [11], $\text{Ca}_2\text{Ti}_3\text{O}_8$ [6], CaTi_2O_5 [12, 13], CaTi_3O_7 [14], $\text{Ca}_2\text{Ti}_5\text{O}_{12}$ [15], and CaTi_4O_9 [16], are mentioned in the literature. They also seem to be unstable, which does not exclude their possible existence [17]. Compiled in this paper on the basis of data [7, 18], as well as the results of recent studies by Gong et al. [19], the phase diagram of the CaO-TiO₂ system in the high-temperature region is shown in **Figure 1**.

2. The thermodynamic properties of perovskite solid phase

Thermochemical data on perovskite [20–24] are based on calorimetric measurements of entropy of perovskite formation $\Delta S_{298}(\text{CaTiO}_3)$, obtained by Shomate [25], and high-temperature heat capacity of perovskite $C_p(\text{CaTiO}_3)$ in the temperature ranges of 15–398 K [26], 293–773 K [27], 376–1184 K [28], 383–1794 K [29], and 413–1825 K [30]. The differences between the data do not exceed 5 J/(mol K) up to a temperature of 1200 K, but they are quite contradictory at higher temperatures (**Figure 2**).

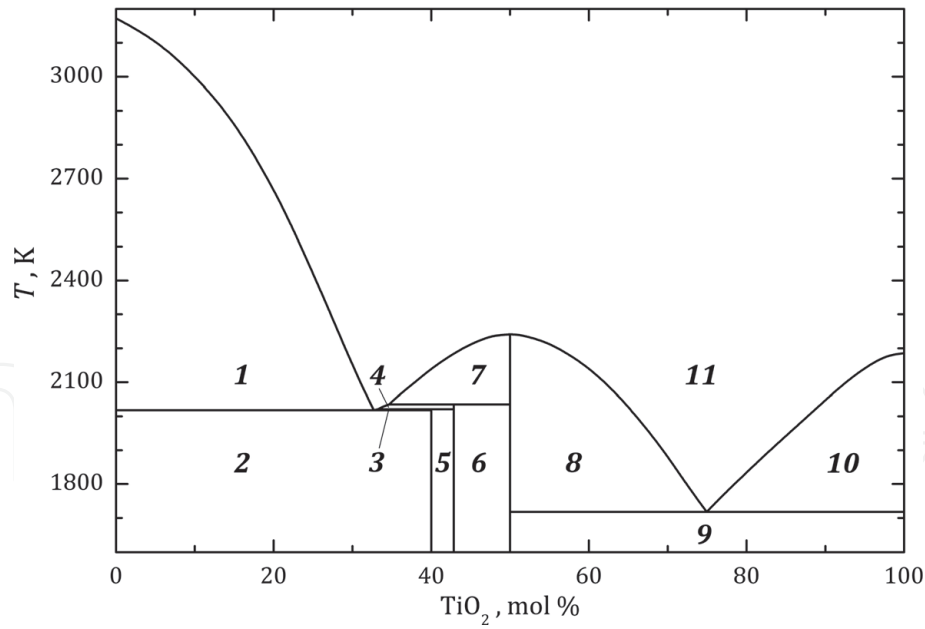


Figure 1.

The phase diagram of the CaO-TiO₂ system [7, 18, 19]: (1) CaO + liquid; (2) CaO + Ca₃Ti₂O₇; (3) Ca₃Ti₂O₇ + liquid; (4) Ca₄Ti₃O₁₀ + liquid; (5) Ca₃Ti₂O₇ + Ca₄Ti₃O₁₀; (6) Ca₄Ti₃O₁₀ + CaTiO₃; (7, 8) CaTiO₃ + liquid; (9) CaTiO₃ + TiO₂; (10) TiO₂ + liquid; (11) liquid.

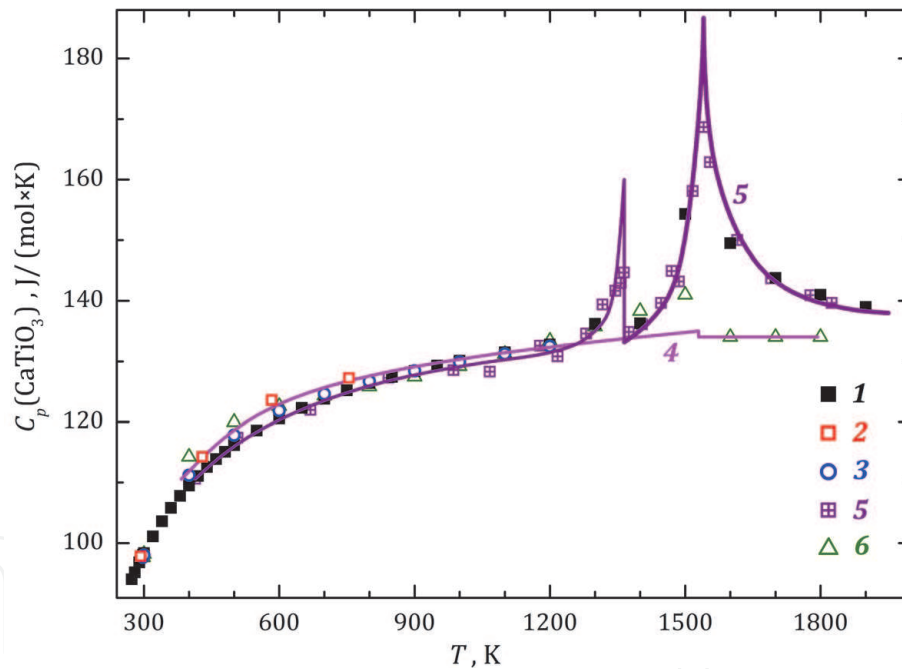


Figure 2.

Heat capacity of perovskite: (1–5) determined via high-temperature calorimetry [26–30], respectively, and (6) taken from [22].

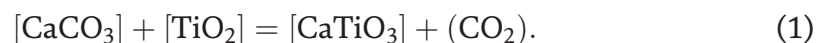
Naylor and Cook [29] determined the enthalpy of perovskite phase transition: 2.30 ± 0.07 kJ/mol at 1530 ± 1 K. The overlapping phase transitions in perovskite observed by Guyot et al. [30] (**Figure 2**) were explained as consequences of a structural change, i.e., a transition from orthorhombic (*Pbnm*) to orthorhombic (*Cmcm*) structure at 1384 ± 10 K and the overlapping of transitions from orthorhombic to tetragonal (*I4/mcm*) and tetragonal to cubic phase (*Pm $\bar{3}m$*) at 1520 ± 10 K with heat effects of 1.0 ± 0.5 and 5.5 ± 0.5 kJ/mol, respectively. The considerable anomaly of perovskite heat capacity above 1520 K could be caused by strong disordering of the cubic phase up to the temperature of perovskite melting. However, based on diffraction data about perovskite structure obtained in the

Experimental approach	T, K	ΔH_T , kJ/mol	ΔS_T , J/(mol K)	Refs.
HF/HCl solution calorimetry	298		1.05 ± 0.21	[25]
HF/HCl solution calorimetry	298	-40.48 ± 0.42	1.86 ± 0.71	[33]
Bomb calorimetry	298	-41.84 ± 1.88		[32]
Adiabatic calorimetry	298	-40.48 ± 1.65	2.40 ± 0.35	[26]
Adiabatic calorimetry	298	-47.11 ± 1.41	2.72 ± 0.23	[28]
Na ₆ Mo ₄ O ₁₅ solution calorimetry	298	-42.98 ± 1.96		[34]
EMF	888–972	-37.05 ± 3.28	4.62 ± 3.54	[35]
EMF	900–1250	-40.07 ± 0.05	3.15 ± 0.05	[36]
Pb ₂ B ₂ O ₅ solution calorimetry	973	-38.73 ± 1.34		[37]
Na ₆ Mo ₄ O ₁₅ solution calorimetry	975	-42.25 ± 1.05		[38]
Na ₆ Mo ₄ O ₁₅ solution calorimetry	975	-41.88 ± 1.36		[39]
Na ₆ Mo ₄ O ₁₅ solution calorimetry	976	-42.86 ± 1.71		[40]
Pb ₂ B ₂ O ₅ solution calorimetry	1046	-42.38 ± 1.82		[37]
(Li,Na)BO ₂ solution calorimetry	1068 ± 2	-40.45 ± 1.15		[41]
Pb ₂ B ₂ O ₅ solution calorimetry	1073	-40.43 ± 1.87	4.37 ± 1.23	[42]
Pb ₂ B ₂ O ₅ solution calorimetry	1074	-43.78 ± 1.73		[43]
Pb ₂ B ₂ O ₅ solution calorimetry	1078	-42.83 ± 3.12		[44]
EMF	1180–1290	-26.88 ± 8.05	11.07 ± 6.44	[45]
Raman spectroscopy	1300		2.82 ± 1.29	[46]
Thermochemical calculations	1600–1800	-37.19 ± 0.14	5.85 ± 0.09	[22]
Thermochemical calculations	1600–2100	-38.23 ± 0.04	5.00 ± 0.02	[23]
Thermochemical calculations	1600–2100	-37.47 ± 0.03	5.60 ± 0.02	[24]
DTA	1740 ± 20	-37.55 ± 3.76		[47]
Knudsen mass spectrometry	1791–2241	-39.98 ± 0.54	3.15 ± 0.28	[48]
Knudsen mass spectrometry	2241–2398	7.73 ± 1.76	24.39 ± 0.76	[48]

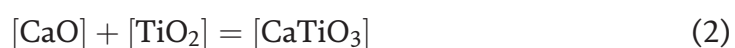
Table 1. Enthalpy and entropy of perovskite formation from simple oxides (calculated per 1 mol of compound).

temperature range of 296–1720 K, Yashima and Ali [31] concluded that the *Cmcm* phase does not exist and claimed that the first transition is the *(Pbnm)* → *(I4/mcm)* at 1512 ± 13 K, followed by the *(I4/mcm)* → *(Pm $\bar{3}m$)* transition at 1635 ± 2 K.

Panfilov and Fedos'ev [32] determined the enthalpy of the reaction with a calorimetric bomb by burning stoichiometric mixtures of rutile TiO₂ and calcium carbonate CaCO₃ (here and below, the square brackets denote the condensed phase; the parentheses denote the gas phase):



They then calculated the enthalpy of perovskite formation $\Delta H_{298}(\text{CaTiO}_3)$: -41.84 ± 1.88 kJ/mol (**Table 1**). Although the obtained value was determined with poor accuracy, due to the difficulty of determining the amounts of substances in the reaction products (1), it corresponded satisfactorily to the more accurate results of Kelley et al. [33], who determined this value according to the reaction:

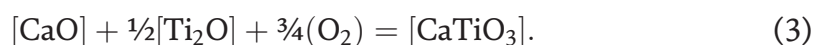


by solution calorimetry in a mixture of hydrofluoric and hydrochloric acids. The reactions of dissolution were more complete than combustion reaction (1).

Navrotsky et al. [19, 26, 34, 37–43] performed a number of studies by various calorimetric methods, using adiabatic calorimetry [26] and solution calorimetry in the (Li, Na)BO₂ [41], Pb₂B₂O₅ [37, 42, 43], and Na₆Mo₄O₁₅ [19, 34, 38–40] salts in the temperature range 973–1074 K. They determined the value of $\Delta H_T(\text{CaTiO}_3)$, which lies in the range of -44 to -39 kJ/mol; the accuracy of measurements was 2 kJ/mol (**Table 1**). The differences could be due to the properties of the solvents that were used. Perovskite and its oxides are poorly soluble in oxide solvent Pb₂B₂O₅; Na₆Mo₄O₁₅ liquid alloy is quite volatile and cannot be used at temperatures above 1000 K; (Li,Na)BO₂ solution is hygroscopic, which creates difficulties in synthesizing [49]. The $\Delta H_{1078}(\text{CaTiO}_3)$ value determined by Koito et al. [44] by similar method (solution calorimetry in Pb₂B₂O₅ salt) is less accurate but close to the results obtained by Navrotsky et al. [19, 34, 37–43].

The data obtained by Sato et al. [28] using adiabatic calorimetry deviate negligibly (by as much as 7 kJ/mol) in the enthalpy values of ($H_T - H_{298}$) in the temperature range above 1000 K. Approximately the same systematic deviation is observed in determination of enthalpy of perovskite formation from oxides (per 1 mole of the compound) due to its use in calculations of the rough semiempirical approximation proposed in [50]. At the same time, the entropy of perovskite formation determined by Sato et al. [28] is in satisfactory agreement with the results obtained by Kelley and Mah [20], Woodfield et al. [26], and Prasanna and Navrotsky [42] and calculated by Gillet et al. [46] based on information obtained on Raman spectra (**Table 1**).

Golubenko and Rezhukhina [45] studied the heterogeneous reaction using a solid electrolyte galvanic cell (EMF method) in the temperature range of 1180–1290 K:



A mixture of FeO and Fe (or NbO and Nb) was used as the reference electrode, and a mixture of La₂O₃-ThO₂ crystals was used as the solid electrolyte. The Gibbs energy of perovskite $\Delta G_T(\text{CaTiO}_3)$ was calculated based on a compilation of fairly approximate literature data and their own estimates of the thermodynamic properties of the [Ti₂O] compound. This produced a considerable error in determining this value (**Figure 3**). Rezhukhina et al. [35] later made more precise measurements of $\Delta G_T(\text{CaTiO}_3)$ in the temperature range of 888–972 K, inside a galvanic cell with CaF₂ as the electrolyte (**Figure 3**). However, the non-systematic errors in determining $\Delta H_T(\text{CaTiO}_3)$ and $\Delta S_T(\text{CaTiO}_3)$ values were considerable (**Table 1**).

Taylor and Schmalzried [51] (at 873 K) and Jacob and Abraham [36] (at 900–1250 K) also determined the perovskite Gibbs energy via EMF using the same solid electrolyte. The obtained $\Delta G_T(\text{CaTiO}_3)$ values were close to the results of Rezhukhina et al. [35].

Klimm et al. [47] used differential thermal analysis (DTA) to determine the enthalpy of reaction (2) at 1740 ± 20 K. The obtained value is consistent with the results of thermochemical calculations, although it has a significant error.

Suito et al. [54, 55] has studied the equilibrium at 1873 K:



in CaO-TiO_x (or CaO-TiO_x-Al₂O₃) slags with liquid nickel, relative to oxygen and nitrogen, depending on the content of Ti (or Al) in the metal. Crucibles made of CaO or Al₂O₃ were used. The activity (a_i) of titanium oxide was estimated indirectly, depending on the content of Al, Ti, and O in the slag, and using data on the Gibbs energies of oxide formation (**Figure 4**).

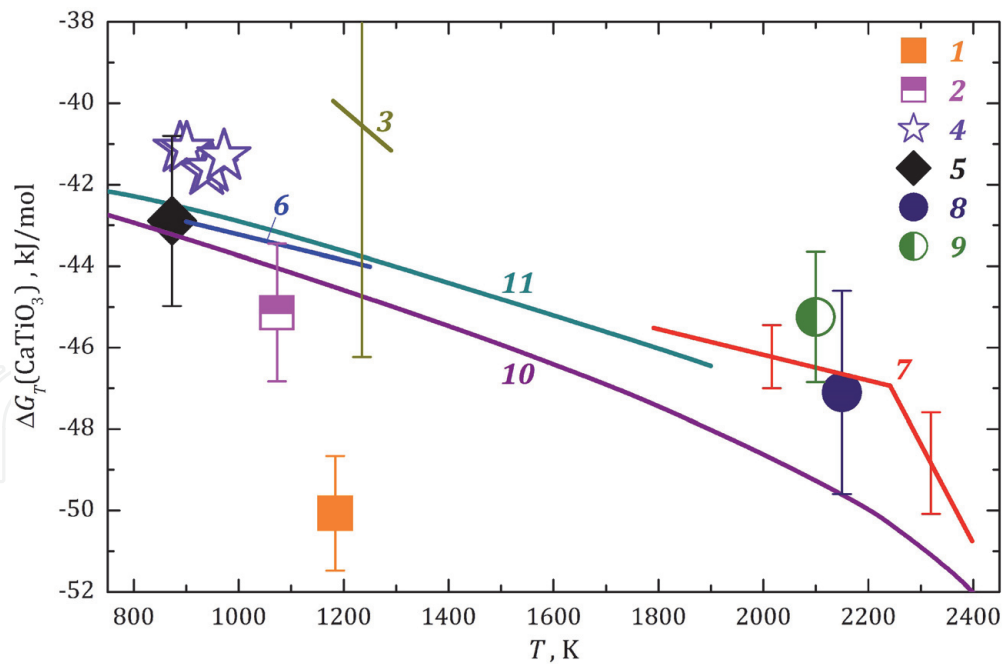


Figure 3.
 The Gibbs energy of the formation of perovskite, determined via (1, 2) calorimetry [28, 42], respectively; (3–6) EMF [35, 36, 45, 51], respectively; (7–9) Knudsen effusion mass spectrometric method in [48, 52, 53], respectively; (10, 11) calculated from thermochemical data in [24, 26], respectively.

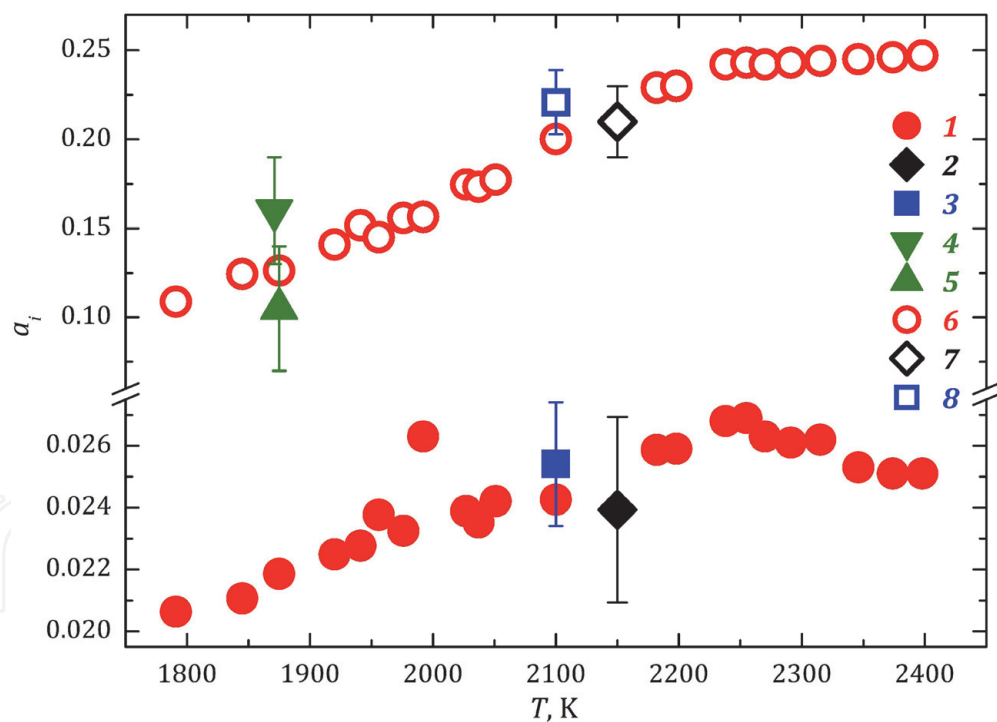


Figure 4.
 Activities of CaO (1–3) and TiO₂ (4–8) in perovskite, determined (1–3, 6–8) via Knudsen effusion mass spectrometry [48, 52, 53] and (4, 5) in studying the heterogeneous equilibria of multicomponent melts [54, 55], respectively.

Banon et al. [52] (at 2150 K) and Shornikov et al. [48, 53, 56] (at 1791–2398 K) determined the values of CaO and TiO₂ activities (**Figure 4**) and $\Delta G_T(\text{CaTiO}_3)$ via Knudsen effusion mass spectrometric method. The resulting values correlated with one another within the experimental error (up to 2.5 kJ/mol); however, the $\Delta G_T(\text{CaTiO}_3)$ was obtained at a temperature ~ 1000 K higher than in the earlier results (**Figure 3**).

As it is seen in **Figure 4**, the values of oxide activities in perovskite determined via Knudsen effusion mass spectrometric method agree with one another in the investigated temperature range. As the temperature grows, there is a slight trend toward the higher activities of calcium and titanium oxides in the crystalline perovskite phase. This trend is less noticeable in the area of the liquid phase. The activities of titanium oxide calculated based on studying of equilibria in slags [54, 55] are fairly approximate but not inconsistent with the results in [48, 52, 53].

The values of Gibbs energy of perovskite formation determined at 800–1200 K via EMF [35, 36, 51] and solution calorimetry [42] correlate satisfactorily with the obtained via Knudsen effusion mass spectrometric method [48, 52, 53, 56]. **Figure 3** shows a good agreement between these data and the results from thermochemical calculations performed by Woodfield et al. [26]. The difference between our findings and the thermochemical data calculated by Bale et al. [24] is large in the perovskite melting area, but is still less than 3 kJ/mol.

The $\Delta H_T(\text{CaTiO}_3)$ and $\Delta S_T(\text{CaTiO}_3)$ values determined in [48] correlate with the results from studies performed via solution calorimetry [37, 41, 42, 44] and EMF [35, 36] at lower temperatures and by Raman spectroscopy [46] and DTA [47] at similar temperatures (**Table 1**).

3. Melting of perovskite

The data characterizing the melting of simple oxides [23, 24, 57–60] are quite rough (**Table 2**). According to different thermochemical data, perovskite's melting temperature lies in the range of 2188 to 2243 K.

Klimm et al. [47] estimated the perovskite melting enthalpy as 56.65 ± 11.33 kJ/mol at 2220 ± 20 K (**Table 2**) which is close to earlier thermochemical estimates [24, 59].

Shornikov [48] based on his own data (**Table 1**) has obtained more accurate values, characterizing the perovskite melting (**Table 2**). They coincide satisfactorily with the experimental data obtained by Klimm et al. [47] and the thermochemical

Compound	T, K	ΔH_{melt} , kJ/mol	ΔS_{melt} , J/(mol K)	References
CaO	2843	52.00	18.29	[59]
	2845	79.50	27.94	[24]
	3200 ± 50	79.50	24.84	[58]
	3210 ± 10	55.20	17.20	[60]
CaTiO ₃	2188	41.84	19.12	[61]
	2220 ± 20	56.65 ± 11.33	25.52 ± 5.10	[47]
	2233	53.32	23.88	[24]
	2241 ± 10	47.61 ± 1.84	21.24 ± 0.81	[48]
	2243	63.65	28.38	[59]
TiO ₂	2103	66.90	31.81	[59]
	2130 ± 20	66.94 ± 16.70	31.43 ± 7.84	[23, 58]
	2130	46.02	21.61	[24]
	2185 ± 10	68.00 ± 8.00	31.12 ± 3.66	[57]

Table 2.

Temperatures, enthalpies, and entropies of the melting of compounds in the CaO-TiO₂ system (calculated for 1 mol of compound)

estimates made by Bale et al. [24]. The enthalpy of perovskite melting estimated using Walden's empirical rule [62] is also close to the result obtained by Shornikov [48]: $\Delta H_{melt} = 8.8$ [J/(g-at K)] $T_{melt} = 49.39$ kJ/mol.

4. The thermodynamic properties of perovskite melts

Thermodynamic information about the CaO-TiO₂ melts is quite scarce and limited by the results of only a few experimental studies. Consider the available experimental data, obtained by the Knudsen effusion mass spectrometry.

Banon et al. [52] investigated the evaporation of 24 compositions of the CaTiO₃-Ti₂O₃-TiO₂ system from molybdenum containers at 1900–2200 K. The synthesized compositions contained up to 90.2 mol% Ti₂O₃ and up to 42 mol% TiO₂ as well as CaTiO₃ compound. Based on the partial vapor pressures (Ca), (TiO), and (TiO₂) over melts at 2150 K, the authors calculated the Ti, TiO, Ti₂O₃, TiO₂, and CaTiO₃ activities, as well as mixing energies in the melts. In the case of the CaTiO₃-TiO₂ melts, the TiO₂ and CaTiO₃ activities were calculated by extrapolation from the data relating to the CaTiO₃-Ti₂O₃-TiO₂ system and thus had, according to the authors themselves, low accuracy, which apparently was caused by inconsistency with different versions of the CaO-TiO₂ phase diagram [7, 9, 11, 18]. Nevertheless Banon et al. [52], interpreting the obtained high values of TiO₂ activities in the region close to titanium dioxide (**Figure 5**), assumed the presence of immiscibility of the CaO-TiO₂ melts in this region.

Stolyarova et al. [63] investigated the properties of the gas phase over 14 compositions of the CaO-TiO₂-SiO₂ system and also determined the values of oxide activity and melt mixing energy by high-temperature mass spectrometry during the evaporation of melts from tungsten effusion containers at 1800–2200 K. The synthesized compositions contained up to 70 mol% CaO, up to 69 mol% SiO₂, and up to 40 mol% TiO₂. As it is shown in **Figure 5**, one of the two studied compositions of the CaO-TiO₂ system at 2057 K was in the “CaO + liquid” region, and thus its value

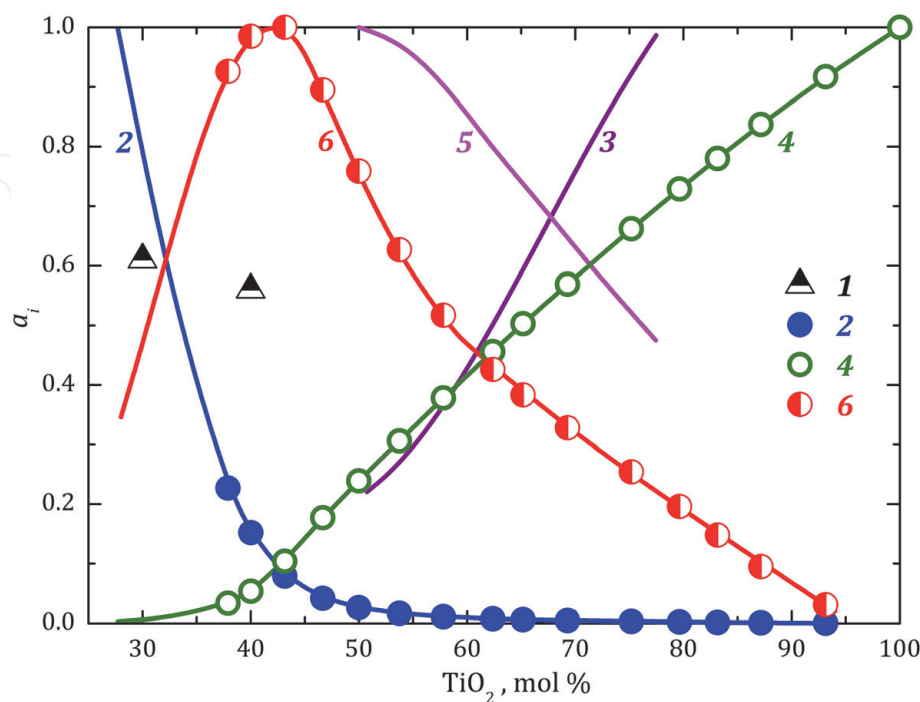


Figure 5.
 The activities of CaO (1, 2), TiO₂ (3, 4), and CaTiO₃ (5, 6) in the CaO-TiO₂ melts, determined at 2057 K (1) in [63], at 2150 K (3, 5) in [52], and at 2250 K (2, 4, 6) in [64].

should be close to 1. The second composition was in the region of “Ca₄Ti₃O₁₀ + liquid,” according to the information presented in [7, 18], or in the region of “Ca₃Ti₂O₇ + liquid,” as follows from the data presented by Tulgar [11]. However, the calculated values are quite close (**Figure 5**), which contradicts the CaO-TiO₂ phase diagram (**Figure 1**). A possible reason for the discrepancies seems to be a significant error in the measurements of CaO activities in the melt, which may be, in our opinion, more than 50%.

Shornikov [64] investigated the evaporation from molybdenum containers of more than 200 compositions of the CaO-TiO₂ system containing from 34 to 98 mol % TiO₂ at 2241–2441 K. The studied compositions were the CaO-TiO₂-SiO₂ residual melts containing up to 1 mol% SiO₂ that was lost during high-temperature evaporation. The determined composition of the gas phase over the CaO-TiO₂ melts allowed to conclude that evaporation reactions are typical for individual oxides predominate.

The oxide activities in the CaO-TiO₂ melts were calculated according to Lewis equations [65]:

$$a_i = p_i/p_i^\circ, \quad (5)$$

where p_i° and p_i are the partial pressures of vapor species over individual oxide and melt, respectively. However, it is preferable to calculate the values of oxide activities using the Belton-Fruehan approach [66] via the following equation:

$$\ln a_i = - \int x_j d \ln (a_j/a_i), \quad (6)$$

in which the ratio of the oxide activities in the melt could be easily converted to the ratio of the partial pressures, proportional to the ion currents (I_i):

$$\begin{aligned} \ln a_{\text{TiO}_2} &= - \int x_{\text{CaO}} d \ln (p_{\text{CaO}}/p_{\text{TiO}_2}) = - \int x_{\text{CaO}} d \ln (p_{\text{Ca}}p_{\text{O}}/p_{\text{TiO}}p_{\text{O}}) \\ &= - \int x_{\text{CaO}} d \ln (I_{\text{Ca}}/I_{\text{TiO}}), \end{aligned} \quad (7)$$

and thus to evade the needs in additional thermochemical data, used in Eq. (5).

The consistency of the values of TiO₂ activities calculated by relation (7) was verified using the Gibbs-Duhem equation [67]:

$$\ln a_{\text{CaO}} = - \int \frac{x_{\text{TiO}_2}}{x_{\text{CaO}}} d \ln a_{\text{TiO}_2}, \quad (8)$$

Values of chemical potentials ($\Delta\mu_i$), partial enthalpy (ΔH_i), and entropy (ΔS_i) of oxides in the CaO-TiO₂ melts were calculated by known equations [67]:

$$\Delta\mu_i = RT \ln a_i \quad (9)$$

$$\Delta\mu_i = \Delta H_i - T\Delta S_i \quad (10)$$

$$\Delta H_i = \frac{d(\Delta\mu_i/T)}{d(1/T)} = R \frac{d \ln a_i}{d(1/T)} \quad (11)$$

$$\Delta S_i = -d\Delta\mu_i/dT, \quad (12)$$

which are related to the corresponding integral thermodynamic mixing functions:

$$\Delta G_T^m = \sum_i x_i \Delta \mu_i \quad (13)$$

$$\Delta H_T = \sum_i x_i \Delta H_i \quad (14)$$

$$\Delta S_T = \sum_i x_i \Delta S_i \quad (15)$$

$$\Delta G_T^m = \Delta H_T - T \Delta S_T \quad (16)$$

and are represented in **Figure 6**.

The results presented by Banon et al. [52] correlate with the data found in [64]. Some difference in values, as mentioned above, is probably due to the procedures for extrapolating information obtained by Banon et al. [52] for compositions of the $\text{CaTiO}_3\text{-Ti}_2\text{O}_3\text{-TiO}_2$ triple system, which could reduce their accuracy. The observed behavior of TiO_2 activity in melts in the concentration region close to rutile may indicate some immiscibility of the melt, which follows from the observed inflection of the concentration dependence (**Figure 5**, line 3). However, in our opinion, the behavior of TiO_2 and CaTiO_3 activities (**Figure 5**, lines 4 and 6) are close to the ideal. The maximum value corresponds to the area of compositions close to

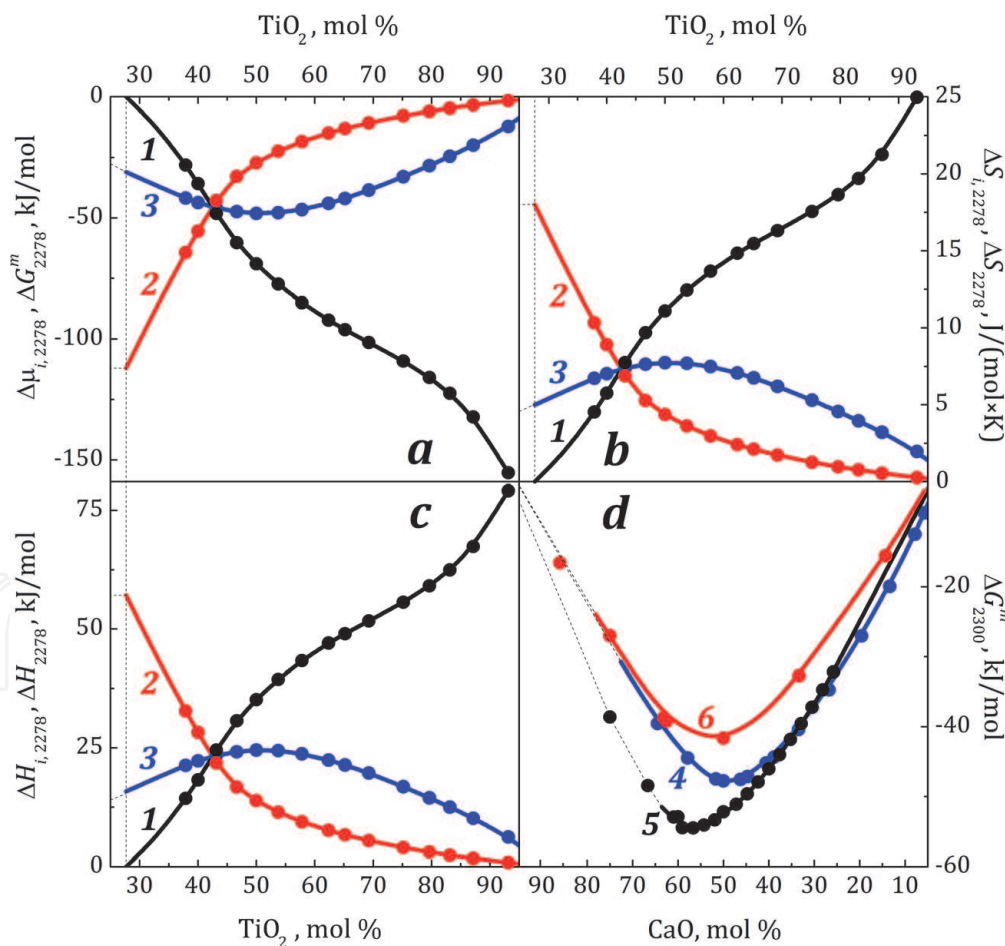


Figure 6.

The thermodynamic properties of the CaO-TiO_2 melts at 2278 K [64] (the chemical potentials of oxides and the mixing energy (a), the partial enthalpies of oxides and the enthalpy of formation (b), and the partial entropies of oxides and the entropy of formation (c)); symbols: (1) CaO , (2) TiO_2 , (3) integral thermodynamic characteristics (mixing energy, enthalpy, and entropy of formation of the melts, respectively); the vertical dashed line marks the boundary of the “ $\text{CaO} + \text{liquid}$ ” region and the melt) and the comparison of mixing energies (d) in the CaO-TiO_2 (4), CaO-SiO_2 (5), and $\text{CaO-Al}_2\text{O}_3$ (6) melts determined by the Knudsen effusion mass spectrometric method in [64, 68, 69], respectively (the dashed lines correspond to heterogeneous areas).

perovskite (**Figure 5**, lines 5 and 6). Differences with values obtained by Stolyarova et al. [63] (**Figure 5**, points 1), are caused, apparently, by the low accuracy of the latter.

The partial and integral thermodynamic regularities presented in **Figure 6** characterizing the CaO-TiO₂ melts are sybatic. The enthalpy and entropy of melt formation are positive. The extreme values of the integral thermodynamic properties of the melts are in the concentration ranges close to perovskite, which confirms its stability in the melt. Some displacement of the extremum of integral thermodynamic functions can be caused by the presence of oxide compounds with a large amount of CaO in comparison with perovskite CaTiO₃ in the melt. A comparison of mixing energies in the CaO-TiO₂ melts at 2300 K with those for the CaO-SiO₂ [68] and CaO-Al₂O₃ [69] melts (**Figure 6d**) indicates a stronger chemical interaction in the CaO-TiO₂ melts than the CaO-Al₂O₃ melts, but smaller than in the CaO-SiO₂ melts. It manifests in more positive values of the mixing energy of the melts.

5. The gas phase over perovskite

The evaporation processes and the thermodynamic properties of simple oxides CaO and TiO₂ were considered in detail in reference books [23, 24, 57, 70, 71].

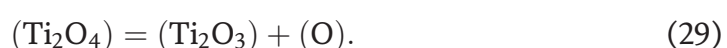
The gas phase over calcium oxide consists of the molecular components (O), (O₂), (O₃), (O₄), (Ca), (Ca₂), and (CaO) possibly formed by the following reactions:



The gas phase over titanium oxide contains similar vapor molecular forms (O), (O₂), (O₃), (O₄), (Ti), (Ti₂), (Ti₃), (TiO), and (TiO₂) formed by similar reactions:



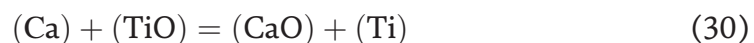
Balducci et al. [72] detected (Ti₂O₃) and (Ti₂O₄) molecules in the gas phase over cobalt titanate CoTiO₃ at 2210–2393 K by the Knudsen effusion mass spectrometric method, which can be involved in the following equilibria:



Note that the predominant components of the gas phase over these oxides are (Ca), (CaO), (TiO), (TiO₂), (O), and (O₂); the content of other vapor species does not exceed 1% of the total concentration at 1700–2200 K.

The properties of the gas phase over perovskite were studied in less detail. The experimental conditions and results of high-temperature studies of perovskite evaporation we will consider below.

Zakharov and Protas [73] studied ion emission from the perovskite surface under the action of laser radiation and identified the ion of a complex molecule (CaTiO₃) in addition to the ions of simple oxides (O⁺, Ca⁺, CaO⁺, Ti⁺, TiO⁺) in the mass spectra of the vapor. They explained the presence of this ion by the similarity of high-temperature evaporation of alkaline-earth oxide titanates, which is confirmed by the composition of the observed condensates (BaTiO₃, SrTiO₃, and CaTiO₃) formed under similar conditions [74, 75]. The intensity ratio of ion currents in the mass spectra of vapor over perovskite obtained at laser pulse duration of 800–1000 μs at a wavelength of 6943 Å and energy of 3–5 J was as follows: $I_{\text{O}}:I_{\text{Ca}}:I_{\text{CaO}}:I_{\text{Ti}}:I_{\text{TiO}}:I_{\text{CaTiO}_3} = 0.41:100:0.17:4.32:0.54:0.05$. Note that the TiO₂⁺ ion was not observed in the mass spectrum of vapor over both perovskite CaTiO₃ and rutile TiO₂. This is explained by the peculiarity of the mass spectrometric experiment using a laser, in which the easily ionizable molecular species dominate the mass spectra of vapor and the not readily ionizable molecules are discriminated. This selectivity of detected ions in the mass spectra of vapor significantly limits the accuracy and applicability of this method [76]. According to the data of [57], the estimated temperature of heating of perovskite under the action of laser radiation based on the possible equilibrium in the gas phase.



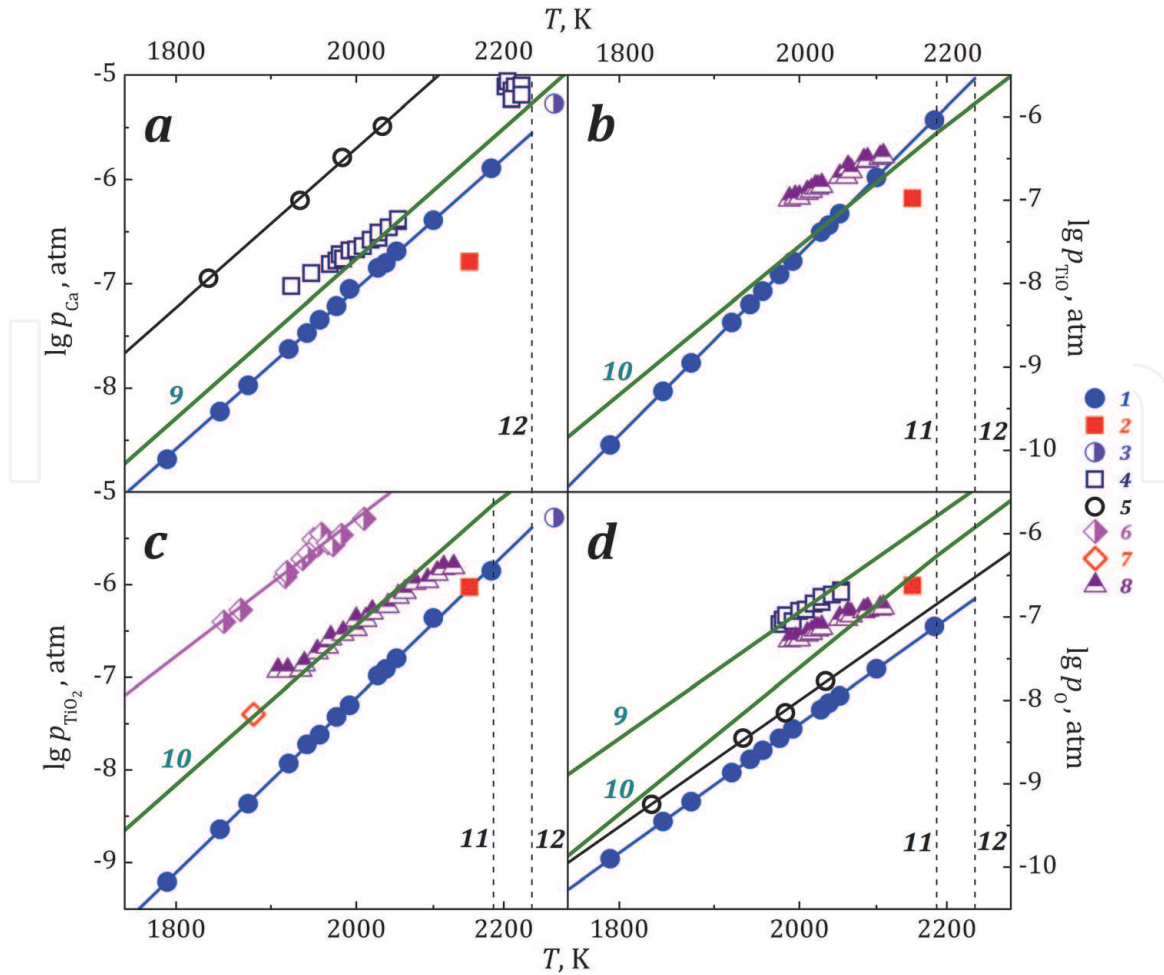
is 4890 ± 70 K, which is approximate, but does not contradict the conditions of similar laser-impact mass spectrometry experiments in the range 4000–6000 K.

Banon et al. [52] studied the evaporation of the CaTiO₃-Ti₂O₃-TiO₂ melts from molybdenum Knudsen effusion cells at 1900–2200 K by differential mass spectrometry. The mass spectra were recorded at a low ionizing voltage of 13 eV in order to avoid possible fragmentation of the TiO₂⁺ molecular ion into Ti⁺ and TiO⁺ fragmentation ions, which were also molecular ions.

Atomic calcium was the dominant component of the gas phase over the composites. The complex gaseous oxide (CaTiO₃) was not detected. The partial pressures of the (Ca), (TiO), (TiO₂), and (O) vapor over perovskite at 2150 K were calculated using the thermochemical data of [57] and are shown in **Figure 7** as a function of the inverse temperature (for easily understanding, the temperature scale was scaled appropriately).

Gaseous perovskite was also not detected in the mass spectrometric studies of high-temperature evaporation of various compositions of the CaO-TiO₂-SiO₂ system from molybdenum and tungsten Knudsen effusion cells at 1700–2500 K [53, 63, 82, 83] presumably because the sensitivity of the equipment used in [63, 83] was insufficient for determining the CaTiO₃⁺ ion or because this was not the purpose of the study [53, 82].

Lopatin and Semenov [84] studied the evaporation of a mixture of calcium carbonate and titanium dioxide from tungsten cells by the Knudsen effusion mass spectrometry method in the temperature range 2100–2500 K. The following ions were detected in the mass spectra of vapor over the mixture: Ca⁺, CaO⁺, Ti⁺, TiO⁺, TiO₂⁺, and CaTiO₃⁺. The energies of ion appearance in the mass spectra allowed the authors to determine the molecular origin of the Ca⁺, CaO⁺, TiO⁺, TiO₂⁺, and CaTiO₃⁺ ions. The TiO⁺ ion also contained a fragment component of the TiO₂⁺ ion,

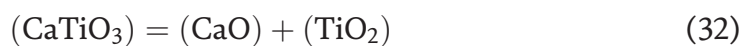

Figure 7.

The partial pressure of Ca (a), TiO (b), TiO₂ (c), and O (d) over perovskite (1–3) and oxides of calcium (4, 5, 9) and titanium (6–8, 10) vs. the inverse temperature, determined via Knudsen mass spectrometry: (1) in [77], (2) in [52], (4) in [78], (5) in [79], (6) in [80], (7) in [81], and (8) in [71]; using the vacuum furnace (according to Langmuir), (3) in [4]; and calculated, (9) and (10), according to the thermochemical data [57]; the vertical dashed lines (11) and (12) indicate melting points of titanium oxide and perovskite, respectively.

and the Ti⁺ ion was completely fragmentary. The energy of appearance of the CaTiO₃⁺ molecular ion was determined to be 9 ± 1 eV (the energy of appearance of the gold ion was used as a standard). The partial pressures of vapor species (p_i) were calculated by comparison with the accepted partial vapor pressures of gold taken as standard pressures (p_s) by the equation:

$$p_i = \frac{I_i T_i}{I_s T_s} p_s \times \frac{\sigma_s \gamma_s \eta_s}{\sigma_i \gamma_i \eta_i}, \quad (31)$$

where I_i (I_s) is the intensity of the ion current of the i th component of vapor (standard substance) recorded at a temperature T_i (T_s). The calculation should also include the ratios of the effective ionization cross sections of the i th molecular form and the standard substance (σ_i/σ_s), isotope distributions (η_i/η_s), and individual ion efficiencies (γ_i/γ_s), which depend on various parameters of ion current recording devices. The pressures p_{CaO} , p_{TiO_2} , and p_{CaTiO_3} calculated by (31) were used to determine the temperature dependence of the equilibrium constant in the gas phase:



Reaction	T, K	$\Delta_f H_{298}$, kJ/mol	$\Delta_f H_T$, kJ/mol	$\Delta_f S_T$, J/(mol K)	Refs.
(CaTiO ₃) = (CaO) + (TiO ₂)	2287–2466	545 ± 8	284 ± 44	28 ± 19	[84]
	2000	—	298 ± 30	—	[85]
	1956–2182	—	287 ± 12	18 ± 6	[77]
[Ca] + [Ti] + 3/2 (O ₂) = (CaTiO ₃)	2287–2466	–826 ± 26	—	—	[84]
	1956–2182	—	–760 ± 10	–242 ± 5	[77]
(CaTiO ₃) = (Ca) + (Ti) + 3(O)	2287–2466	2225 ± 26	—	—	[84]
	2000	—	1983 ± 81	—	[85]
	1956–2182	—	1993 ± 15	396 ± 7	[77]
[CaTiO ₃] = (CaTiO ₃)	2000	—	1030 ± 22	—	[85]
	1956–2182	—	1027 ± 10	297 ± 5	[77]

Table 3.
 Enthalpies and entropies of the reactions involving the CaTiO₃ molecule.

and subsequently calculate the enthalpies of formation ($\Delta_f H_{298}$) and atomization ($\Delta_{at} H_{298}$) of the CaTiO₃ molecule (**Table 3**).

Zhang et al. [4] studied the isotope fractionation of calcium and titanium during the evaporation of a perovskite melt suspended on an iridium wire in a vacuum furnace at a temperature of 2278 K (according to Langmuir method). The change in the composition of the residual perovskite melt during evaporation suggested that the component that evaporated predominantly from the melt was its calcium component. The total vapor pressure over perovskite could be evaluated from the data obtained (**Figure 7**).

Shornikov [64, 77] investigated the evaporation of perovskite at 1791–2182 K and its melts at 2241–2441 K from molybdenum Knudsen effusion cells by high-temperature mass spectrometric method.

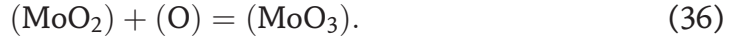
The TiO₂⁺, Ca⁺, TiO⁺, and O⁺ ions prevailed in the mass spectra of vapor over perovskite and its melts at the ionizing electron energy of 20 eV, as well as other ions characteristic of the mass spectra over individual oxides [57, 58, 71]. A small amount of CaTiO₃⁺ ion was observed, which was fragmented into CaTi⁺, CaTiO⁺, and CaTiO₂⁺ ions ($I_{CaTi}:I_{CaTiO}:I_{CaTiO_2}:I_{CaTiO_3} = 6:10:13:100$). The ratio of the ion current intensities in the mass spectra of vapor over perovskite at 2182 K was the following: $I_{Ca}:I_{CaO}:I_{Ti}:I_{TiO}:I_{TiO_2}:I_{CaTiO_3}:I_{O}:I_{O_2} = 80:0.04:0.1:75:100:0.02:40:0.3$. It corresponded to that observed by Samoilova and Kazenas [78] in the same temperature range at evaporation of CaO from alundum cell and by Semenov [86] at evaporation of TiO₂ from a tungsten cell.

The ratio of the ion current intensities in the mass spectra of vapor over perovskite melt containing 57.81 ± 0.15 mol% TiO₂ at 2278 K was the following: $I_{Ca}:I_{CaO}:I_{Ti}:I_{TiO}:I_{TiO_2}:I_{CaTiO_3}:I_{O}:I_{O_2} = 25:0.02:0.1:56:100:0.13:0.44:0.012$, which is different from that for the case of perovskite [77].

The presence of MoO_i⁺ ($i = 0-3$) ions in the mass spectra of vapor over perovskite was due to the evaporation of molybdenum cell at high temperature:

$$[Mo] = (Mo), \quad (33)$$

as well as the interaction of perovskite with the cell material ($I_{TiO_2}:I_{Mo}:I_{MoO}:I_{MoO_2}:I_{MoO_3} = 100:0.8:2.6:7.3:0.6$) that was detected according to the following equilibria:



Note that Berkowitz et al. [81] found that during evaporation of titanium oxide from a molybdenum liner inserted into a tantalum crucible at 1881 K, p_{MoO_2} was initially $10\text{--}10^2$ times higher than p_{TiO_2} . The p_{MoO_2} value gradually decreased and became comparable with the p_{TiO_2} value, which is significantly different from the other results [52, 53, 56, 64, 77, 82]. The high p_{MoO_2} observed in [81] probably was due to poor quality of the molybdenum liner material (or its alloy). Possibly it was made using powder technology from MoO_3 reduced to metal molybdenum at ~ 1300 K. It could lead to such an excess of partial pressure of (MoO_3) and its decrease as it evaporates from the surface layers of the liner material.

The appearance energies of ions in the mass spectra of vapor over perovskite were determined by the Warren method [87] and corresponded to the accepted values of the ionization energies of atoms and molecules [88]. The appearance energy of CaTiO_3^+ ion in the mass spectra of vapor over perovskite was equal to 8.5 ± 0.6 eV (the appearance energy of silver ion was used as a standard) and corresponded to obtained by Lopatin and Semenov [84].

The established molecular composition of the gas phase over perovskite allowed us to draw a conclusion on the predominant evaporation of perovskite according to the reactions (17), (18), (20), (23), (24), and (25), typical for evaporation of simple oxides [57, 71, 78, 86]. The presence of a small amount of (CaTiO_3) molecules in the gas phase over perovskite is probably due to the reaction:



The partial pressure values of vapor species in the gas phase over perovskite were determined by the Hertz-Knudsen equation, written in the following form [89]:

$$p_i = K_\alpha \frac{q_i}{s_{or} C_{or} t} \sqrt{\frac{2\pi RT}{M_i}}, \quad (38)$$

where q_i is the amount of i th substance component evaporated from the effusion cell, M_i is the molecular weight, t is time of evaporation, T is temperature, C_{or} is the Clausing coefficient characterized the effusion hole, and s_{or} is the hole area.

The K_α constant value was calculated taking into account the evaporation coefficient (α_i) of substance component associated with the molecule changing during its transition to the gas phase from the surface with an S_v area, using the Komlev equation [90]:

$$K_\alpha = \frac{1}{C_{or}} + s_{or} \frac{1 - C_c \alpha_i}{S_v \alpha_i C_c}, \quad (39)$$

where C_c is the Clausing coefficient characterized effusion cell.

The Clausing coefficient is associated with the collision of vapor species inside the effusion orifice channel of effusion cell and their reverse reflection from the channel walls. Its value does not exceed 1 and depends on the ratio of the diameter of the effusion hole to its thickness.

Taking into account predominance of typical for CaO and TiO₂ vapor species in the gas phase over perovskite and small amounts of CaTiO₃, the α_i values were used from [91].

The partial pressures of vapor species over perovskite at 1791–2182 K and its melts at 2278 K calculated using the relationships (38) and (39) with an error not exceeding 8% are shown in **Figure 8**.

The partial pressure of atomic oxygen determined using the relationships (38) and (39) agrees satisfactorily with those calculated using the thermochemical data [57] on $K_r(T)$ equilibrium constants of possible reactions (18), (20), (24), (25), and (36) in the gas phase over perovskite in the following relations:

$$p_{\text{O}} = \frac{p_{\text{CaO}}}{p_{\text{Ca}}} K_{18}(T) \quad (40)$$

$$p_{\text{O}} = \frac{p_{\text{TiO}_2}}{p_{\text{TiO}}} K_{24}(T) \quad (41)$$

$$p_{\text{O}} = \frac{p_{\text{TiO}}}{p_{\text{Ti}}} K_{25}(T) \quad (42)$$

$$p_{\text{O}} = \sqrt{\frac{p_{\text{O}_2}^2}{K_{20}(T)}} \quad (43)$$

$$p_{\text{O}} = \frac{p_{\text{MoO}_3}}{p_{\text{MoO}_2}} K_{36}(T). \quad (44)$$

It should be noted that the p_{O} values calculated according to the independent reactions in the gas phase over perovskite (40)–(45) were the same. It confirmed the assumption about the molecular origin of the identified ions in the mass spectrum of vapor over perovskite.

As it follows from **Figure 8a**, the defined partial pressures of vapor species over perovskite can be represented as linear logarithmic dependence vs. the inverse temperature:

$$\lg p_i = a_i/T + b_i. \quad (45)$$

Note that the relationship (45) is the same as the expression for the reaction constant [57]:

$$R \ln K_r(T) = -\frac{\Delta_r G_T}{T} = -\frac{\Delta_r H_T}{T} + \Delta_r S_T, \quad (46)$$

which allows to determine the enthalpy ($\Delta_r H_T$) and entropy ($\Delta_r S_T$) of a reaction.

The partial pressures of the predominant vapor species of the gas phase over perovskite (Ca, TiO, TiO₂ and O) are compared in **Figure 7** with the results on evaporation of simple oxides (CaO and TiO₂) under similar redox conditions caused by the interaction of oxygen with molybdenum [79, 81], tungsten [71], and tantalum [80] effusion cells or in chemically neutral conditions (in the absence of this interaction) for alundum cell [78].

We used the TiO and TiO₂ activities as well as the Gibbs energy of perovskite obtained by Banon et al. [52] and thermochemical data [52] on equilibriums (17), (18), (23), and (24) to estimate the partial pressure of vapor species over the perovskite at 2150 K. Therefore, the obtained values characterized by the evaporation of perovskite were not under reducing conditions (from molybdenum cell),

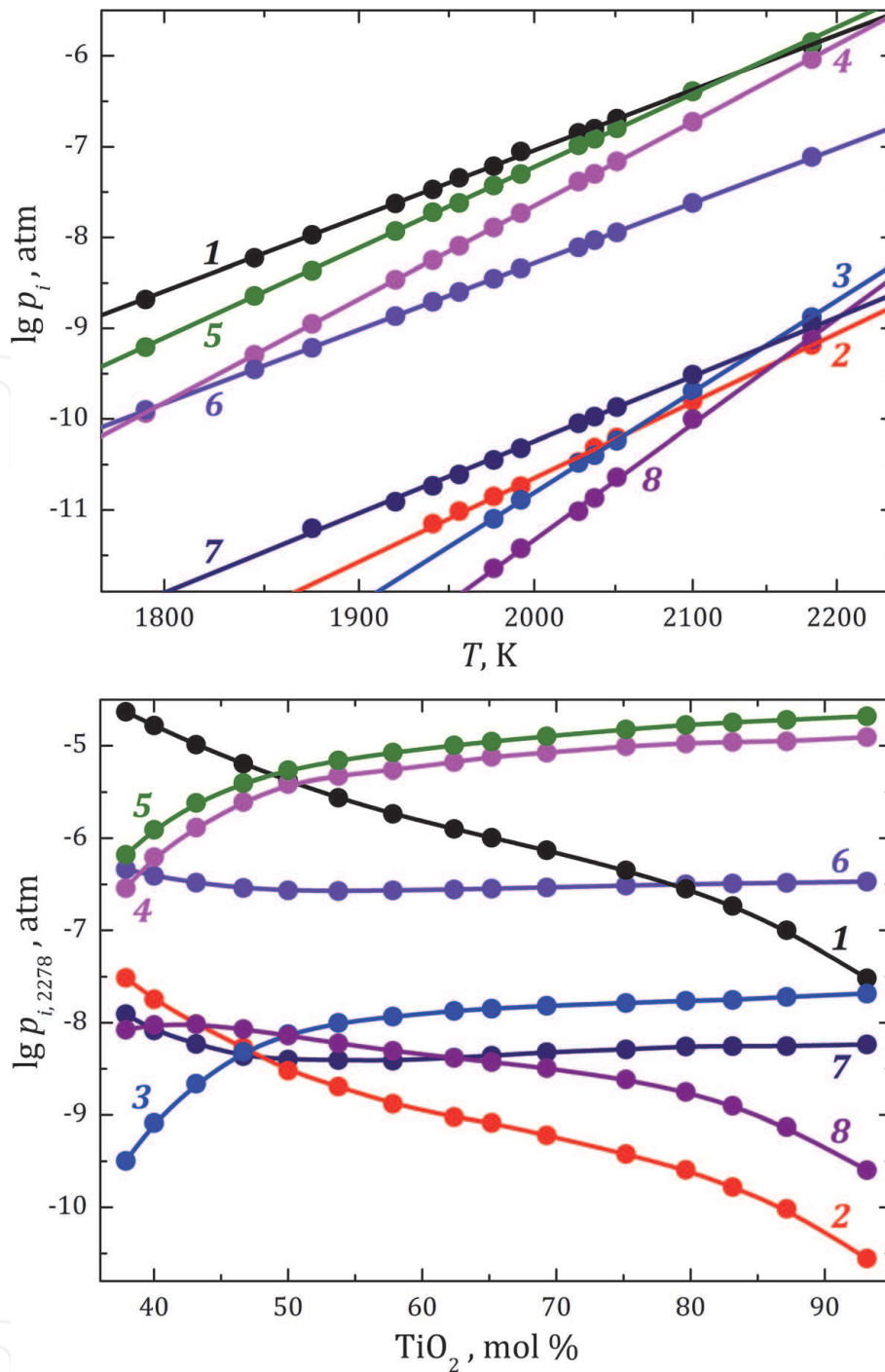


Figure 8.

The partial pressure values of vapor species over perovskite (a) [77] and over the CaO-TiO_2 melts at 2278 K (b) [64]: (1) Ca, (2) CaO, (3) Ti, (4) TiO, (5) TiO_2 , (6) O, (7) O_2 , and (8) CaTiO_3 .

but, in contrary, under chemically neutral conditions (in the absence of interaction of perovskite with the cell material).

Figure 7 also shows the partial pressures of vapor species over calcium and titanium oxides calculated using thermochemical data [57]. By comparison of the experimental data obtained in [71, 77–81] and the calculated results, we can see the effect of reducing properties of cell materials on gas phase composition: tantalum [80], molybdenum [79, 81], tungsten [71], and alundum [78]. As we noted earlier [85], the greatest effect of cell materials on the vapor composition are observed with the oxygen-“deficient” species such as atomic calcium (**Figure 7a**), titanium monoxide (**Figure 7b**), and atomic oxygen itself (**Figure 7d**). There are no differences in the partial pressure of gaseous titanium dioxide (**Figure 7c**) determined in evaporation experiments using molybdenum [81] and tungsten [71] cells.

The total vapor pressure over the perovskite melt at 2278 K obtained by Zhang et al. [4] is consistent with the extrapolated values of partial pressures of the predominant vapor species of the gas phase—atomic calcium and titanium dioxide (**Figure 7a** and **c**) found in [77].

Similar slopes of $\lg p_{\text{Ca}}$ and $\lg p_{\text{O}}$ vs. the inverse temperature for calcium oxide and perovskite in **Figure 7a** and **d** (lines 1, 5 and 9, respectively) indicate a predominant effect of calcium component on evaporation of calcium from perovskite. This also can explain the difference in the slope of $\lg p_{\text{TiO}}$ in **Figure 7b** in the case of perovskite (line 1) and rutile (line 10) according to the equilibriums (18) and (24).

The enthalpy and entropy of reactions involving CaTiO_3 gaseous complex oxide calculated by the relationship (46) are given in **Table 3**. They are in a good agreement with those found by Lopatin and Semenov [84] and our earlier estimates [85].

The concentration dependences of partial pressures of vapor species over perovskite melts show a sharp decrease in p_{Ca} and p_{CaO} (**Figure 8b**, lines 1 and 2) with increasing of TiO_2 content in the melt. The vapor species containing titanium—(Ti), (TiO), and (TiO_2) —are increased with increasing TiO_2 concentration up to 65–70 mol% TiO_2 , and further they are almost constant in the region of 75–100 mol% TiO_2 (**Figure 8b**, lines 3–5), which may indicate the immiscibility of the melt observed by Banon et al. [52]. The partial pressures of (O) and (O_2) slightly vary throughout the concentration range under consideration, showing a minimum in the perovskite concentration (**Figure 8b**, lines 6 and 7). The (CaTiO_3) partial pressures have maximum values in the melt region with a high calcium content compared to the perovskite concentration (**Figure 8b**, line 8), as it was noted earlier.

6. Conclusions

The thermodynamic properties of perovskite determined by different calorimetric approaches and EMF method agree with the results obtained via Knudsen effusion mass spectrometry at high temperatures. The resulting values of oxide activities in perovskite, as well as the Gibbs energy, the entropy and enthalpy of the formation of perovskite from simple oxides, and the melting enthalpy of perovskite are consistent with each other. The enthalpy of perovskite formation is constant throughout the temperature range, and the entropy of perovskite formation tends to increase slightly.

The oxide activities in perovskite melts were determined by mass spectrometric Knudsen effusion method. The thermodynamic properties of melts (chemical potentials of oxides and mixing energies, as well as partial and integral enthalpies and entropies of melt's formation) were calculated based on the experimental data. The obtained experimental information testifies to the sybante behavior of thermodynamic functions characterizing the melts. The extreme values of the integral thermodynamic properties of melts are in the concentration region close to perovskite, which confirms its stability in the melt. The displacement of the extremum of the integral thermodynamic functions in the CaO-TiO_2 melts can be caused by the presence in the melt of oxide compounds with a large amount of CaO compared to perovskite. A comparison of mixing energies in the CaO-TiO_2 melts with those for the CaO-SiO_2 and $\text{CaO-Al}_2\text{O}_3$ melts indicates a stronger chemical interaction in the CaO-TiO_2 melts than the similar $\text{CaO-Al}_2\text{O}_3$ melts, but smaller than in the CaO-SiO_2 melts.

The evaporation of perovskite and its melts from a molybdenum cell at high temperature was studied by the Knudsen effusion mass spectrometric method. The molecular components typical of simple oxides and the (CaTiO_3) gaseous complex

oxide were identified in the gas phase over perovskite. The partial vapor pressures of the molecular components of the gas phase over perovskite were determined. A comparison of these values with the available experimental data and with the values corresponding to simple oxides showed that the character of perovskite evaporation is mainly affected by the calcium component of perovskite. The observed concentration dependences of the partial pressures of vapor species over the perovskite melts correspond to those characterizing the condensed phase.

Acknowledgements

This study was financially supported by the Presidium of the Russian Academy of Sciences (Program No. 7 “Experimental and Theoretical Studies of Solar System and Star Planetary System Objects. Transition Processes in Astrophysics”) and by the Russian Foundation for Basic Research (Grant No. 19-05-00801A “Thermodynamics of Formation Processes of Substance of Refractory Inclusions in Chondrites”).

Thanks

I am grateful to Oleg Yakovlev (Vernadsky Institute of Geochemistry and Analytical Chemistry of the Russian Academy of Sciences) for his constant interest in this study and useful discussions and to Mikhail Nazarov (Vernadsky Institute of Geochemistry and Analytical Chemistry of the Russian Academy of Sciences) for his support during this work. I express my special gratitude to Marina Ivanova (Vernadsky Institute of Geochemistry and Analytical Chemistry of the Russian Academy of Sciences; National Museum of Natural History of Smithsonian Institution) for her help in working on the manuscript.


Author details

Sergey Shornikov

Vernadsky Institute of Geochemistry and Analytical Chemistry of Russian Academy of Sciences, Moscow, Russia

*Address all correspondence to: sergey.shornikov@gmail.com

IntechOpen

© 2020 The Author(s). Licensee IntechOpen. This chapter is distributed under the terms of the Creative Commons Attribution License (<http://creativecommons.org/licenses/by/3.0>), which permits unrestricted use, distribution, and reproduction in any medium, provided the original work is properly cited. 

References

- [1] Rose G. Über einige neue mineralien des Urals. *Journal für Praktische Chemie*. 1840;**19**:459-468
- [2] Stefanovsky SV, Yuditsev SV. Titanates, zirconates, aluminates and ferrites as waste forms for actinide immobilization. *Russian Chemical Reviews*. 2016;**85**:962-994
- [3] Wark D, Boynton WV. The formation of rims on calcium-aluminum-rich inclusions: Step I—Flash heating. *Meteoritics & Planetary Science*. 2001;**36**:1135-1166
- [4] Zhang J, Huang S, Davis AM, Dauphas N, Hashimoto A, Jacobsen SB. Calcium and titanium isotopic fractionations during evaporation. *Geochimica et Cosmochimica Acta*. 2014;**140**:365-380
- [5] Ivanova MA. Ca-Al-rich inclusions in carbonaceous chondrites: The oldest solar system objects. *Geochemistry International*. 2016;**54**:387-402
- [6] Parga Pondal I, Bergt K. Sobre la combinacion de la cal en los sistemas CaO–TiO₂ y CaO–SiO₂–TiO₂. *Anales de la Sociedad Española de Física y Química*. 1933;**31**:623-637
- [7] Roth RS. Revision of the phase equilibrium diagram of the binary system calcia–titania, showing the compound Ca₄Ti₃O₁₀. *Journal of Research of NBS*. 1958;**61**:437-440
- [8] Lazaro SR. Estudo teorico-experimental do titanato de calcio—CaTiO₃ [thesis]. Sao Carlos: Universidade Estadual Paulista, Instituto de Quimica; 2002. p. 57
- [9] Wartenberg HV, Reusch HJ, Saran E. Schmelzpunktsdiagramme hochstfeuerfester oxyde. VII. Systeme mit CaO und BeO. *Zeitschrift für Anorganische und Allgemeine Chemie*. 1937;**230**:257-276
- [10] Pontes FM, Pinheiro CD, Longo E, Leite ER, Lazaro SR, Varela JA, et al. The role of network modifiers in the creation of photoluminescence in CaTiO₃. *Materials Chemistry and Physics*. 2003;**78**:227-233
- [11] Tulgar HE. Solid state relationships in the system calcium oxide—Titanium dioxide. *Istanbul Teknik Üniversitesi Bülteni*. 1976;**29**:111-129
- [12] Kisel NG, Limar TF, Cherednichenko IF. On calcium dititanate. *Russian Journal of Inorganic Chemistry*. 1972;**8**:1782-1785
- [13] Pfaff G. Peroxide route to synthesize calcium titanate powders of different composition. *Journal of the European Ceramic Society*. 1992;**9**:293-299
- [14] Seko A, Hayashi H, Kashima H, Tanaka I. Matrix- and tensor-based recommender systems for the discovery of currently unknown inorganic compounds. *Physical Review Materials*. 2018;**2**:13805-1-13805-9
- [15] Savenko VG, Sakharov VV. Formation of calcium titanate Ca₂Ti₅O₁₂ on thermolysis of mixed titanium and calcium hydroxides. *Russian Journal of Inorganic Chemistry*. 1979;**24**:1389-1391
- [16] Limar TF, Kisel NG, Cherednichenko IF, Savos'kina AI. On calcium tetratitanate. *Russian Journal of Inorganic Chemistry*. 1972;**17**:559-561
- [17] Oganov AR, Ma Y, Lyakhov AO, Valle M, Gatti C. Evolutionary crystal structure prediction as a method for the discovery of minerals and materials. *Reviews in Mineralogy and Geochemistry*. 2010;**71**:271-298

- [18] DeVries RC, Roy R, Osborn EF. Phase equilibria in the system CaO–TiO₂. *The Journal of Physical Chemistry*. 1954;**58**:1069-1073
- [19] Gong W, Wu L, Navrotsky A. Combined experimental and computational investigation of thermodynamics and phase equilibria in the CaO–TiO₂ system. *Journal of the American Ceramic Society*. 2018;**101**:1361-1370
- [20] Kelley KK, Mah AD. Metallurgical thermochemistry of titanium. U. S. Bur. Min. Repts. 1959. No. 5490. 48 p
- [21] Reznitskii LA, Guzei AS. Thermodynamic properties of alkaline earth titanates, zirconates, and hafnates. *Russian Chemical Reviews*. 1978;**47**:99-119
- [22] Robie RA, Hemingway BS. Thermodynamic properties of mineral and related substances at 298.15 K and 1 bar (105 Pascals) pressure and high temperatures. U. S. Geol. Surv. Bull. 1995. No. 2131. p. 461
- [23] Barin I. Thermochemical Data of Pure Substances. VCH: Weinheim; 1995. p. 2003
- [24] Bale CW, Belisle E, Chartrand P, Decterov SA, Eriksson G, Gheribi AE, et al. FactSage thermochemical software and databases, 2010–2016. *Calphad*. 2016;**54**:35-53
- [25] Shomate CH. Heat capacities at low temperatures of the metatitanates of iron, calcium and magnesium. *Journal of the American Chemical Society*. 1946;**68**:964-966
- [26] Woodfield BF, Shapiro JL, Stevens R, Boerio-Goates J, Putnam RL, Helean KB, et al. Molar heat capacity and thermodynamic functions for CaTiO₃. *The Journal of Chemical Thermodynamics*. 1999;**31**:1573-1583
- [27] Buykx WJ. Specific heat, thermal diffusivity and thermal conductivity of synroc, perovskite, zirconolite and barium hollandite. *Journal of Nuclear Materials*. 1982;**107**:78-82
- [28] Sato T, Yamazaki S, Yamashita T, Matsui T, Nagasaki T. Enthalpy and heat capacity of (Ca_{1-x}Pu_x)TiO₃ ($x = 0$ and 0.20). *Journal of Nuclear Materials*. 2001;**294**:135-140
- [29] Naylor BF, Cook OA. High-temperature contents of the metatitanates of calcium, iron and magnesium. *Journal of the American Chemical Society*. 1946;**68**:1003-1005
- [30] Guyot F, Richet P, Courtial P, Gillet P. High-temperature heat capacity and phase transitions of CaTiO₃ perovskite. *Physics and Chemistry of Minerals*. 1993;**20**:141-146
- [31] Yashima M, Ali R. Structural phase transition and octahedral tilting in the calcium titanate perovskite CaTiO₃. *Solid State Ionics*. 2009;**180**:120-126
- [32] Panfilov BI, Fedos'ev NN. Heat of formation of metatitanate calcium, strontium and barium. *Russian Journal of Inorganic Chemistry*. 1964;**9**:2685-2692
- [33] Kelley KK, Todd SS, King EG. Heat and free energy data for titanates of iron and the alkaline-earth metals. U. S. Bur. Min. Repts. 1954. No. 5059. p. 37
- [34] Feng D, Shivaramaiah R, Navrotsky A. Rare-earth perovskites along the CaTiO₃–Na_{0.5}La_{0.5}TiO₃ join: Phase transitions, formation enthalpies, and implications for loparite minerals. *American Mineralogist*. 2016;**101**:2051-2056
- [35] Rezukhina TN, Levitskii VA, Frenkel' MY. Thermodynamic properties of barium and calcium tungstates. *Russian Inorganic Materials*. 1966;**2**:325-331

- [36] Jacob KT, Abraham KP. Thermodynamic properties of calcium titanates: CaTiO_3 , $\text{Ca}_4\text{Ti}_3\text{O}_{10}$, and $\text{Ca}_3\text{Ti}_2\text{O}_7$. *The Journal of Chemical Thermodynamics*. 2009;**41**:816-820
- [37] Putnam RL, Navrotsky A, Woodfield BF, Boerio-Goates J, Shapiro JL. Thermodynamics of formation for zirconolite ($\text{CaZrTi}_2\text{O}_7$) from $T = 298.15 \text{ K}$ to $T = 1500 \text{ K}$. *The Journal of Chemical Thermodynamics*. 1999;**31**:229-243
- [38] Navi NU, Shneck RZ, Shvareva TY, Kimmel G, Zabicky J, Mintz MH, et al. Thermochemistry of $(\text{Ca}_x\text{Sr}_{1-x})\text{TiO}_3$, $(\text{Ba}_x\text{Sr}_{1-x})\text{TiO}_3$, and $(\text{Ba}_x\text{Ca}_{1-x})\text{TiO}_3$ perovskite solid solutions. *Journal of the American Ceramic Society*. 2012;**95**:1717-1726
- [39] Sahu SK, Maram PS, Navrotsky A. Thermodynamics of nanoscale calcium and strontium titanate perovskites. *Journal of the American Ceramic Society*. 2013;**96**:3670-3676
- [40] Helean KB, Navrotsky A, Vance ER, Carter ML, Ebbinghaus B, Krikorian O, et al. Enthalpies of formation of Ce-pyrochlore, $\text{Ca}_{0.93}\text{Ce}_{1.00}\text{Ti}_{2.035}\text{O}_{7.00}$, U-pyrochlore, $\text{Ca}_{1.46}\text{U}_{0.23}^{4+}\text{U}_{0.46}^{6+}\text{Ti}_{1.85}\text{O}_{7.00}$ and Gd-pyrochlore, $\text{Gd}_2\text{Ti}_2\text{O}_7$: Three materials relevant to the proposed waste form for excess weapons plutonium. *Journal of Nuclear Materials*. 2002;**303**:226-239
- [41] Takayama-Muromachi E, Navrotsky A. Energetics of compounds ($\text{A}^{2+}\text{B}^{4+}\text{O}_3$) with the perovskite structure. *Journal of Solid State Chemistry*. 1988;**72**:244-256
- [42] Prasanna TRS, Navrotsky A. Energetics in the brownmillerite-perovskite pseudobinary $\text{Ca}_2\text{Fe}_2\text{O}_5$ - CaTiO_3 . *Journal of Materials Research*. 1994;**9**:3121-3124
- [43] Linton J, Navrotsky A, Fei Y. The thermodynamics of ordered perovskites on the CaTiO_3 - FeTiO_3 join. *Physics and Chemistry of Minerals*. 1998;**25**:591-596
- [44] Koito S, Akaogi M, Kubota O, Suzuki T. Calorimetric measurements of perovskites in the system CaTiO_3 - CaSiO_3 and experimental and calculated phase equilibria for high-pressure dissociation of diopside. *Physics of the Earth and Planetary Interiors*. 2000;**120**:1-10
- [45] Golubenko AN, Rezhukhina TN. Thermodynamic properties of calcium titanate from electrochemical measurements at elevated temperatures. *Russian Journal of Physical Chemistry*. 1964;**38**:2920-2923
- [46] Gillet P, Guyot F, Price GD, Tournerie B, LeCleach A. Phase changes and thermodynamic properties of CaTiO_3 . Spectroscopic data, vibrational modelling and some insights on the properties of MgSiO_3 perovskite. *Physics and Chemistry of Minerals*. 1993;**20**:159-170
- [47] Klimm D, Schmidt M, Wolff N, Gugushev C, Ganschow S. On melt solutions for the growth of CaTiO_3 crystals. *Journal of Crystal Growth*. 2018;**486**:117-121
- [48] Shornikov SI. High-temperature mass spectrometric study of the thermodynamic properties of CaTiO_3 perovskite. *Russian Journal of Physical Chemistry A*. 2019;**93**:1428-1434
- [49] Topor ND, Suponitskii YL. The high-temperature microcalorimetry of inorganic substances. *Russian Chemical Reviews*. 1984;**53**:827-850
- [50] Aronson S. Estimation of the heat of formation of refractory mixed oxides. *Journal of Nuclear Materials*. 1982;**107**:343-346
- [51] Taylor RW, Schmalzried H. The free energy of formation of some titanates,

- silicates and magnesium aluminate from measurements made with galvanic cells involving solid electrolyte. *The Journal of Physical Chemistry*. 1964;**68**:2444-2449
- [52] Banon S, Chatillon C, Allibert M. Free energy of mixing in $\text{CaTiO}_3\text{-Ti}_2\text{O}_3\text{-TiO}_2$ melts by mass spectrometry. *Canadian Metallurgical Quarterly*. 1981; **20**:79-84
- [53] Shornikov SI, Archakov IY. Mass spectrometric study of thermodynamic properties of the $\text{SiO}_2\text{-CaTiO}_3$ melts. In: Kudin L, Butman M, Smirnov A, editors. *Proc. II Intern. Symp. on High Temperature Mass Spectrometry*. Ivanovo: ISUCST; 2003. pp. 112-116
- [54] Cho SW, Suito H. Thermodynamics of oxygen and nitrogen in liquid nickel equilibrated with CaO-TiO_x and $\text{CaO-TiO}_x\text{-Al}_2\text{O}_3$ melts. *Metallurgical and Materials Transactions A*. 1994;**25**:5-13
- [55] Kishi M, Suito H. Thermodynamics of oxygen, nitrogen and sulfur in liquid iron equilibrated with CaO-TiO_x and $\text{CaO-TiO}_x\text{-Al}_2\text{O}_3$ melts. *Steel Research*. 1994;**65**:261-266
- [56] Shornikov SI, Archakov IY, Shultz MM. Thermodynamic properties of the melts, containing titanium dioxide. In: Gorynin IV, Ushkov SS, editors. *Proc. 9th World Conf. on Titanium*. Vol. 3. Saint-Petersburg: Prometey; 2000. pp. 1469-1473
- [57] Glushko VP, Gurvich LV, Bergman GA, Veitz IV, Medvedev VA, Khachkuruzov GA, et al. *Thermodynamic Properties of Individual Substances*. Moscow: Nauka; 1978-1982 [in Russian]
- [58] Chase MW. NIST-JANAF thermochemical tables. *Journal of Physical and Chemical Reference Data*. 1998. p. 1951
- [59] Nerad I, Danek V. Thermodynamic analysis of pseudobinary subsystems of the system $\text{CaO-TiO}_2\text{-SiO}_2$. *Chemical Papers*. 2002;**56**:77-83
- [60] Seo W-G, Zhou D, Tsukihashi F. Calculation of thermodynamic properties and phase diagrams for the CaO-CaF_2 , BaO-CaO and BaO-CaF_2 systems by molecular dynamics simulation. *Materials Transactions*. 2005;**46**:643-650
- [61] Bottinga Y, Richet P. Thermodynamics of liquid silicates, a preliminary report. *Earth and Planetary Science Letters*. 1978;**40**:382-400
- [62] Kulikov IS. *Thermal Dissociation of Compounds*. 2nd ed. Metallurgiya: Moscow; 1969. p. 576 [in Russian]
- [63] Stolyarova VL, Zhegalin DO, Stolyar SV. Mass spectrometric study of the thermodynamic properties of melts in the $\text{CaO-TiO}_2\text{-SiO}_2$ system. *Glass Physics and Chemistry*. 2004;**30**: 142-150
- [64] Shornikov SI. Thermodynamic properties of CaO-TiO_2 system: Experimental data and calculations. In: Gladyshev PP, editor. *Physical and Analytical Chemistry of Natural and Technogenic Systems, New Technologies and Materials—Khodakovsky's Readings*. Dubna: Dubna State University; 2019. pp. 185-190 [in Russian]
- [65] Lewis GN, Randall M. *Thermodynamics and the Free Energy of Chemical Substances*. N. Y. & London: McGraw-Hill Book Comp.; 1923. p. 676
- [66] Belton GR, Fruehan RJ. The determination of activities of mass spectrometry: Some additional methods. *Metallurgical and Materials Transactions B*. 1971;**2**:291-296
- [67] Prigogine I, Defay R. *Chemical Thermodynamics*. London: Longman; 1954. p. 543

- [68] Shornikov SI, Archakov IY. Mass spectrometric study of phase relations and vaporization processes in the CaO–SiO₂ system. *Glass Science and Technology: International Journal of the German Society of Glass Technology*. 2000;**73C2**:51-57
- [69] Shornikov SI, Stolyarova VL, Shultz MM. A mass-spectrometric study of vapor composition and thermodynamic properties of CaO–Al₂O₃ melts. *Russian Journal of Physical Chemistry*. 1997;**71**:19-22
- [70] Kulikov IS. *Thermodynamics of Oxides*. Metallurgiya: Moscow; 1986. p. 344 [in Russian]
- [71] Kazenas EK, Tsvetkov YV. *Evaporation of Oxides*. Moscow: Nauka; 1997. p. 543 [in Russian]
- [72] Balducci G, Gigli G, Guido M. Identification and stability determinations for the gaseous titanium oxide molecules Ti₂O₃ and Ti₂O₄. *The Journal of Chemical Physics*. 1985;**83**:1913-1916
- [73] Zakharov VP, Protas IM. Mass spectrometric study of ion emission during evaporation of complex substances under the influence of laser radiation. *Izvestiya Akademii Nauk SSSR. Seriya Fizicheskaya (Bulletin of the Russian Academy of Sciences: Physics)* 1974;**38**:238-243
- [74] Schwarz H, Tourltellotte HA. Vacuum deposition by high-energy laser with emphasis on barium titanate films. *Journal of Vacuum Science and Technology B*. 1969;**6**:373-378
- [75] Hao J, Si W, Xia XX, Guo R, Bhalla AS, Cross LE. Dielectric properties of pulsed-laser-deposited calcium titanate thin films. *Applied Physics Letters*. 2000;**76**:3100-3102
- [76] Knox BE. Laser ion source analysis of solids. In: Ahearn AJ, editor. *Trace Analysis by Mass Spectrometry*. N. Y. & London: Academic Press; 1972. pp. 423-444
- [77] Shornikov SI. Mass-spectrometric study of perovskite evaporation. *Russian Journal of Physical Chemistry A*. 2019;**93**:866-873
- [78] SamoiloVA IO, Kazenas EK. Thermodynamics of dissociation and sublimation of calcium oxide. *Russel Metals*. 1995:33-35
- [79] Shornikov SI. *Evaporation processes and thermodynamic properties of the CaO–Al₂O₃–SiO₂ system and the materials based on this system [thesis]*. Institute of Silicate Chemistry of RAS: Saint-Petersburg; 1993. p. 21 [in Russian]
- [80] Groves WO, Hoch M, Johnston HL. Vapor–solid equilibria in the titanium–oxygen system. *The Journal of Physical Chemistry*. 1955;**59**:127-131
- [81] Berkowitz J, Chupka WA, Inghram MG. Thermodynamics of the Ti–Ti₂O₃ system and the dissociation energy of TiO and TiO₂. *The Journal of Physical Chemistry*. 1957;**61**:1569-1572
- [82] Archakov IY, Shornikov SI, Tchemekova TY, Shultz MM. The behavior of titanium dioxide in the slag melts. In: Gorynin IV, Ushkov SS, editors. *Proc. 9th World Conf. on Titanium*. Vol. 3. Saint-Petersburg: Prometey; 2000. pp. 1464-1468
- [83] Ostrovski O, Tranell G, Stolyarova VL, Shultz MM, Shornikov SI, Ishkildin AI. High-temperature mass spectrometric study of the CaO–TiO₂–SiO₂ system. *High Temperature Materials and Processes*. 2000;**19**:345-356
- [84] Lopatin SI, Semenov GA. Thermochemical study of gaseous salts of oxygen-containing acids: XI. Alkaline-earth metal titanates. *Russ. J. General Chemistry*. 2001;**71**:1522-1526

[85] Shornikov SI, Yakovlev OI. Study of complex molecular species in the gas phase over the CaO–MgO–Al₂O₃–TiO₂–SiO₂ system. *Geochemistry International*. 2015;**53**:690-699

[86] Semenov GA. The evaporation of titanium dioxide. *Russian Inorganic Materials*. 1969;**5**:67-73

[87] Warren JW. Measurement of appearance potentials of ions produced by electron impact, using a mass spectrometer. *Nature*. 1950;**165**:810-811

[88] Gurvich LV, Karachevtsev GV, Kondratev VN, Lebedev YA, Medvedev VA, Potapov VK, et al. *Bond Dissociation Energies, Ionization Potentials, and Electron Affinity*. Moscow: Nauka; 1974. p. 351
[in Russian]

[89] Shornikov SI. Thermodynamic study of the mullite solid solution region in the Al₂O₃–SiO₂ system by mass spectrometric techniques. *Geochemistry International*. 2002;**40**:S46-S60

[90] Komlev GA. On determination of saturated steam pressure by effusion method. *Russian Journal of Physical Chemistry*. 1964;**38**:2747-2748

[91] Shornikov SI. Vaporization coefficients of oxides contained in the melts of Ca-Al-inclusions in chondrites. *Geochemistry International*. 2015;**53**:1080-1089